

ADMarker: A Multi-Modal Federated Learning System for Monitoring Digital Biomarkers of Alzheimer’s Disease

Xiaomin Ouyang¹, Xian Shuai¹, Yang Li¹, Li Pan¹, Xifan Zhang¹, Heming Fu¹, Xinyan Wang¹, Shihua Cao¹, Jiang Xin¹, Hazel Mok¹, Zhenyu Yan¹, Doris Sau Fung Yu¹, Timothy Kwok¹, Guoliang Xing^{1,*}

¹The Chinese University of Hong Kong

*Corresponding Author

ABSTRACT

Alzheimer’s Disease (AD) and related dementia are a growing global health challenge due to the aging population. In this paper, we present ADMarker, the first end-to-end system that integrates multi-modal sensors and new federated learning algorithms for detecting multidimensional AD digital biomarkers in natural living environments. ADMarker features a novel three-stage multi-modal federated learning architecture that can accurately detect digital biomarkers in a privacy-preserving manner. Our approach collectively addresses several major real-world challenges, such as limited data labels, data heterogeneity, and limited computing resources. We built a compact multi-modality hardware system and deployed it in a four-week clinical trial involving 91 elderly participants. The results indicate that ADMarker can accurately detect a comprehensive set of digital biomarkers with up to 93.8% accuracy and identify early AD with an average of 88.9% accuracy. ADMarker offers a new platform that can allow AD clinicians to characterize and track the complex correlation between multidimensional interpretable digital biomarkers, demographic factors of patients, and AD diagnosis in a longitudinal manner.

1 INTRODUCTION

Alzheimer’s Disease (AD) is a progressive neurodegenerative disease that can cause significantly declining cognitive and functional abilities. AD and related dementia is a growing health challenge worldwide because of population aging [32, 33]. In 2010, about 35.6 million people lived with dementia, which is expected to double every 20 years [20].

A major barrier to the treatment of AD is that many patients are either not diagnosed or diagnosed at the late stages of the disease. Studies suggest that 75% of worldwide persons with dementia are undiagnosed [1]. This is largely due to the fact that, the standard clinical procedure for AD diagnosis,

based on Magnetic Resonance Imaging (MRI), Positron Emission Tomography (PET) brain scan, or blood biomarkers like amyloid β_{1-42} , is only available in clinical settings. Although various screening tests can identify cognitive impairments, they are usually intrusive and cannot be conducted routinely or in a real-time manner. Therefore, early identification of people at risk of developing AD and timely intervention to slow the onset and progression of AD are crucial.

A recent major advance in early AD diagnosis and intervention is to leverage AI and sensor devices to capture physiological, behavioral, and lifestyle symptoms of AD (e.g., activities of daily living and social interactions) in natural home environments, referred to as *digital biomarkers* [2, 22, 27]. The difficulty in performing activities of daily living (ADLs) is a hallmark feature of AD, because ADLs, such as watching TV, cleaning living areas, and taking medicine, involve tasks that require independence, organization, judgment, and sequencing abilities [57]. Moreover, social behaviors, such as family meals and phone calls, are shown to be strongly correlated with the risk of early AD [11, 19].

There are several major challenges that have not been addressed in previous work on AD digital biomarkers. First, existing work is focused on a particular type of digital biomarker, such as motor function [17, 29], speech features [35, 44], or driving habits [12], which lacks generalizability to subjects with various demographic and medical characteristics. Second, most of the studies are based on the black-box approach, where the sensor data/feature is directly used to identify AD, which will not only incur extremely high computing overhead but also result in digital biomarkers that are difficult to interpret by medical professionals.

In this paper, we present ADMarker, the first end-to-end system that integrates multi-modal sensors and new federated learning (FL) algorithms for detecting multidimensional, more than 20 AD digital biomarkers in a privacy-preserving

	Approach	Accuracy	# of biomarkers	Sensors	# of subjects	Duration
Tatc [29]	Black-box, Centralized	42.3% for MCI	1 (sensor data)	Actigraphy	729 (185 AD, 103 MCI, 441 NC)	7 days
ADReSS [35]	Black-box, Centralized	60.8% for AD	6 acoustic features	Audio	156 (78 AD, 78 non-AD)	10mins (in lab)
Bayat et al. [12]	Black-box, Centralized	82% fro AD	14 GPS driving indicators	In-vehicle GPS	139 (64 AD, 75 non-AD)	One year
Alberdi et al. [9]	Interpretable, Centralized	No diagnosis results	Features of 5 events	PIR motion sensor	29 (6 AD, 10 MCI, 12 NC)	Two years
ADMarker (Ours)	Interpretable, Distributed	88.9% for MCI	Features of 22 activities	Audio, Depth, Radar	91 (31 AD, 30 MCI, 30 NC)	Four weeks

Table 1: Comparison of different AD digital biomarker studies. ADMarker is the first solution that detects a comprehensive set of multidimensional digital biomarkers for AD diagnosis in a privacy-preserving manner.

manner. The system features a novel three-stage FL architecture, where the nodes deployed in subjects’ homes leverage the pre-trained model to reduce the compute overhead of online training, and improve the model performance on their own data through multi-modal unsupervised and weakly supervised FL algorithms. This approach collectively addresses several real-world challenges, including limited labeled data, data heterogeneity and variation, and limited computing resources. We have implemented ADMarker on a compact multi-modality sensor hardware system with three privacy-preserving sensors (i.e., a depth camera, a mmWave radar, and a microphone) to detect a comprehensive set of digital biomarkers in home environments. To ensure durability and efficiency, the design of ADMarker addresses several practical challenges in the hardware and software system, including long-term multi-modal data recording, improving training and inference efficiency, and private communication networks.

We have deployed ADMarker in a four-week clinical trial that involves a total of 91 elderly subjects, including 31 with AD and 30 with mild cognitive impairment (MCI). The results show that, ADMarker can detect more than 20 daily activities in natural home environments with up to 93.8% detection accuracy, using only a very small amount of labeled data. Leveraging the detected digital biomarkers, we can achieve 88.9% accuracy in early AD diagnosis. ADMarker offers a new clinical tool that allows medical researchers and professionals to monitor the progression of AD manifestations and study the complex correlation between multidimensional interpretable digital biomarkers, demographic factors of patients, and AD diagnosis in a longitudinal manner.

2 RELATED WORK

Mobile Health Systems. Numerous mobile health systems have been proposed in recent years [15, 16, 24, 34, 54]. Recently, several mobile systems are developed for the assessment or rehabilitation of neurodegenerative diseases. For example, NeuralGait [28] captures the gait segments relationship for brain health assessment. PDLens [64] uses the smartphone data for drug-effectiveness detection of Parkinson’s disease. However, these systems can only monitor very limited symptoms of the disease, e.g., the gait or sound of the subjects. ADMarker is the first system that can detect

multi-dimensional AD digital biomarkers in a real-time and privacy-preserving manner.

Federated Learning for Human Activity Recognition. Machine learning algorithms have been increasingly adopted for Human Activity Recognition (HAR) [25, 56, 62]. Most work in this space is based on centralized learning that needs to train the algorithms at a central server, which imposes significant privacy concerns due to the need to share raw user data. Moreover, current HAR studies are focused on classifying a small number of activities in controlled environments. Federated learning (FL) has been recently applied to HAR to improve the model accuracy without sharing the raw data [47, 48, 59]. However, most of the existing FL approaches are focused on training *unimodal* models with a single type of sensor data. Several multi-modal federated learning schemes [46, 65] allow model training over distributed multi-modal data on the nodes. However, they have not addressed the unique challenges in real-world multi-modal federated learning, such as limited labels and modality heterogeneity. ADMarker is the first multi-modal FL system that incorporates novel unsupervised and weakly supervised multi-modal FL designs to detect a comprehensive set of human activities in natural living environments.

Digital Biomarkers for Alzheimer’s Disease. Recently, understanding AD using mobile sensor-based digital biomarkers has attracted tremendous attention [12, 17, 27, 29, 35]. Table 1 compares several representative AD digital biomarker studies. In summary, these studies have two key major issues. First, they are focused on a very small number of activities, such as sitting, sleeping, and eating. As a result, the detected digital biomarkers are only applicable to partial population demographics or environments. Second, most of the studies are based on the black-box approach that directly infers the diagnosis from raw sensor data/features. Such an approach incurs extremely high computing overhead, as the amount of collected data over time can be huge (e.g., about 90T in our four-week clinical deployment). In addition, even if the diagnosis with raw sensor data is accurate, the results are difficult to interpret with respect to AD manifestations. As a result, they are difficult to be adopted in current practices of AD diagnosis and treatment that are largely based on observable cognitive and behavioral symptoms [2, 27].

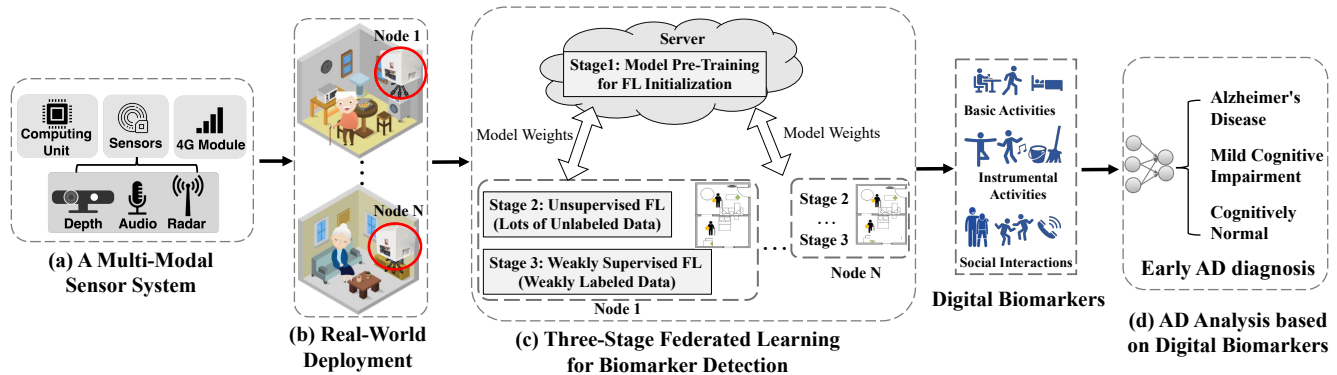


Figure 1: Overview of ADMarker. ADMarker consists of three major components, i.e., a multi-modal sensor system, federated learning algorithms for biomarker detection, and AD analysis based on detected digital biomarkers.

3 SYSTEM OVERVIEW

3.1 Motivation

Interpretable two-step AD monitoring. Instead of predicting AD with the raw multi-modal sensor data (i.e., black-box approaches in Table 1), ADMarker disentangles the disease monitoring into two steps, i.e., digital biomarkers (AD symptoms) detection and early disease analysis with the detected biomarkers. As a result, the behavior biomarkers detected by ADMarker are more interpretable for AD diagnosis and can be adopted to design personalized intervention plans for different individuals.

Detecting multi-dimensional biomarkers. Compared with existing approaches focused on a particular type of digital biomarker [12, 29, 35], ADMarker aims to detect a comprehensive set of multi-dimensional AD symptoms, such as various activities of daily living and social interactions. This allows to investigate how the physical and social interactional etiopathogenesis shape AD’s manifestation. Furthermore, the integration of multi-dimensional digital biomarkers enables the precise detection of early AD, encompassing its diverse manifestations, which would be challenging when relying solely on a single type of biomarker [32, 33].

Federated learning for privacy-preserving biomarker detection. To continuously and accurately detect the biomarkers, ADMarker needs to accumulate data for a certain period of time and use it to train machine learning models for daily activity recognition. In order to preserve users’ data privacy, ADMarker features a federated learning [26, 47] paradigm for biomarker detection, which only requires the nodes to upload model weights to avoid exposing users’ raw data during the learning process.

3.2 Challenges

ADMarker aims to address three major challenges:

The first challenge is to *utilize a large set of digital biomarkers for early AD diagnosis and intervention*. It is essential to

select a comprehensive set of activities that are highly associated with different AD stages yet can be detected accurately during daily life. This requires extensive domain expertise in both medical and engineering areas.

The second challenge is to develop *a hardware system that can be rapidly deployed in real-world home environments* for longitudinal daily activity monitoring. For instance, in order to capture multi-dimensional digital biomarkers in a privacy-preserving manner, the hardware system should incorporate carefully selected sensors of different modalities.

The third challenge is to design *an effective multi-modal federated learning system that can accurately detect digital biomarkers* under real-world data and system dynamics. First, there usually exists no labels or only a very limited amount of labeled data in real-world settings because most sensor data is not intuitive for humans to label [53]. Second, due to the significant diversity in behavior patterns and home environments, the data distribution of different subjects is usually non-i.i.d. and highly imbalanced. For instance, compared with cognitively normal subjects, AD patients tend to have a sedentary lifestyle. As a result, they may have very limited data for activities like “exercising” and “cleaning the living area”, while these activities are as important as frequently occurring activities like “sitting” for AD analysis. Finally, there may be significant training latency in real-world FL systems due to the limited computing resources and dynamic bandwidth of nodes.

3.3 System Architecture

Our key idea is to leverage multi-modal sensor devices and federated learning algorithms to detect multi-dimensional AD digital biomarkers in natural home environments. Figure 1 shows the overview of ADMarker.

We developed a compact multi-modality hardware system that can function for up to months in home environments to detect digital biomarkers of AD. It incorporates three privacy-preserving sensors (a depth camera, an mmWave

Class Index	Activities	Captured Sensors	Type	Decline at which stage
1	Out of Home	Depth, Radar, Mic		Mild, Moderate
2	Other activities	Depth, Radar, Mic		
3	Dressing	Depth, Radar	BADL	Moderate, Severe
4	Take/Put something	Depth, Radar	BADL	Severe
5	Cleaning living area	Depth, Radar, Mic	IADL	Mild
6	Grooming	Depth, Radar	IADL	Moderate, Severe
7	Wiping hands	Depth, Radar	BADL	Severe
8	Drinking	Depth, Radar	BADL	Moderate, Severe
9	Eating	Depth, Radar, Mic	BADL	Moderate, Severe
10	Smoking	Depth, Radar	IADL	Mild
11	Sneezing/Coughing	Depth, Radar, Mic	BADL	Mild
12	Writing	Depth, Radar	IADL	Mild
13	Watching TV	Depth, Radar, Mic	BADL	Mild
14	Phone call/Using phone	Depth, Radar, Mic	SI	Mild
15	Exercising	Depth, Radar	IADL	Moderate, Severe
16	Talking with others	Depth, Radar, Mic	SI	Severe
17	Stretching	Depth, Radar	BADL	Mild, Moderate
18	Walking	Depth, Radar	BADL	Moderate, Severe
19	Sitting	Depth, Radar	BADL	Moderate, Severe
20	Standing	Depth, Radar	BADL	Severe
21	Lying	Depth, Radar	BADL	Moderate, Severe
22	Moving in/out of chair	Depth, Radar	IADL	Severe

Table 2: Selected AD digital biomarkers. BADL: Basic Activities of Daily Living; IADL: Instrumental Activities of Daily Living; SI: Social Interaction.

radar, and a microphone), an NVIDIA single-board edge computer, and a 4G cellular interface that can communicate with the server. We address several practical challenges to make the hardware system durable, power-efficient, and privacy-preserving. On top of the hardware system, we design a new multi-modal federated learning (FL) system for biomarker detection while preserving users’ data privacy. The system features a novel three-stage architecture. At the first stage, we train a multi-modal model on the server using the labeled data from public datasets or the previous participants. Then, during the deployment, the nodes in the subjects’ homes will load the centrally pre-trained model, and improve the model performance on their own data through a two-stage FL process, i.e., multi-modal unsupervised and weakly supervised FL, respectively. In weakly supervised FL, the nodes will only leverage *weak labels* generated from sparse activity logs of the participants, without resorting to labor-intensive manual annotation of raw sensor data, for local model training. Our approach collectively addresses several major real-world challenges, including limited labeled data, data heterogeneity, and limited computing resources. Finally, the digital biomarkers are input into a neural network for AD diagnosis of different patients.

The design of ADMarker is extensively evaluated in a clinical deployment (see Section 7). A total of 91 elderly subjects (43 females and 48 males, 61-93 years old) were recruited for the study, including 31 with AD, 30 with mild cognitive impairment, and 30 cognitively normal subjects.

3.4 Biomarker Selection

We select a total of 22 activities of interest that are shown to be highly related to AD from medical literature [10, 13, 36, 37]. ADMarker will detect these activities and use the duration and frequency of the activities as potential digital biomarkers for diagnostic analysis (see Section 8.4).

Table 2 shows the activities in the biomarker set, which can be categorized into three types: *basic activities of daily living (BADLs)*, *instrumental activities of daily living (IADLs)*, and *social interactions (SI)*. BADLs include basic self-care tasks, such as eating, drinking, and walking, while IADLs encompass complex tasks that allow for independent living, like cleaning the living area and grooming [10, 50]. AD patients who suffer from decreased ability in ADLs and social interactions are more likely to exhibit amyloid plaques and neurofibrillary tangles in several brain regions [36, 37].

Moreover, the last column in Table 2 shows the stages of the disease where these activities become difficult for the patients. At the mild stage of AD, activities like watching TV [23] and using phone [63] become challenging due to early signs of cognitive decline. When the disease progresses to moderate and severe stages, the patients will suffer comprehensive functional deterioration, and are difficult to perform basic activities like standing [42], exercising [41], and talking with others [40]. Therefore, the digital biomarkers selected above are not only interpretable with respect to AD manifestations, but also can be readily applied in intervention plans. For example, by monitoring the subjects’ daily activities during the progression of AD, the duration and intensity of exercise can be prescribed for personalized intervention, which leads to iterative and more effective treatment.

4 FEDERATED LEARNING FOR BIOMARKER DETECTION

4.1 A Motivation Study

4.1.1 Understanding the real-world challenges. We first analyze the sensor data and system log recorded by our ADMarker testbed (see Section 6) in a four-week clinical deployment to understand the real-world challenges.

Data challenges. Figure 2 shows the examples of data distributions of participants over the four weeks of the clinical deployment (see Section 7). First, the amount of data from different activities is highly imbalanced. For example, in the daily living activities of Subject 3, the ratio of samples from class 1 (Out of Home, 81.78%) is very large, while that from class 15 (Exercising, 1.54%) is small. The imbalanced activity distribution will lead to a model bias on head classes, and a significant classification accuracy drop on minority tail classes [31, 52]. Second, the distributions of different subjects’ data are non-i.i.d. For example, the number of occurred activities and their ratios are very different between

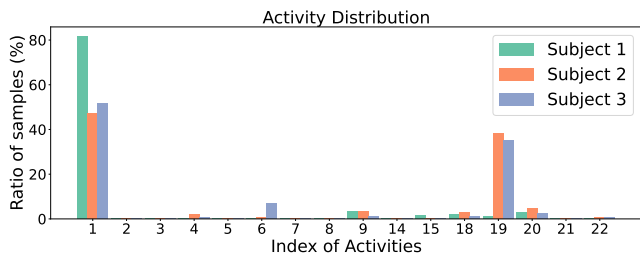


Figure 2: Examples of data distributions of participants in a real-world deployment. The data distribution is highly imbalanced among different classes and non-i.i.d across different participants.

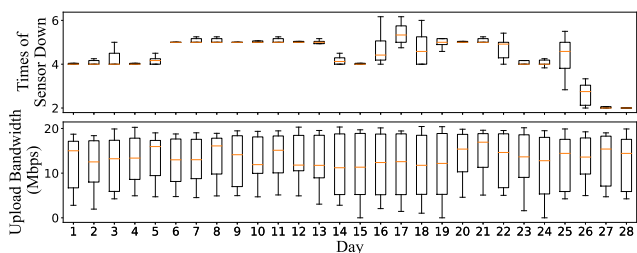


Figure 3: Times of sensor down and bandwidth of all nodes over four weeks of the real-world deployment.

Subject 1 (cognitively normal) and Subject 3 (AD). The non-i.i.d data distribution across nodes will reduce the accuracy performance during FL [47, 48]. For example, the accuracy of federated learning reduces by up to 55% for models trained for highly skewed non-i.i.d data [66]. Finally, there usually exists no labels or only a very small amount of labeled data in real-world settings because the sensor data (depth images, radar point cloud, and MFCC audio features in ADMarker) is not intuitive for humans to label (as shown in Figure 7c).

System dynamics. We then evaluate the long-term system dynamics using the system log recorded during the real-world deployment. The results are shown in Figure 3. The upper sub-figure shows the down times of sensors (per day) of the ADMarker prototype over four weeks, where each box shows the statistics of all nodes in the day. During the 4-week deployment, the sensors may stop data recording occasionally (about 2-6 times per day) due to the system dynamics, such as power surges or unstable sensor connections, resulting in heterogeneous sensor modalities across different nodes in FL. The lower sub-figure shows the upload bandwidth of nodes (with 4G LTE networks) over different days, which fluctuates in a significant dynamic range (e.g., 0-20 Mbps). Such bandwidth dynamics will result in various communication delays in transmitting model weights in federated learning.

Approach	Pre-trained	Supervised	Semi-supervised
Training data	N/A	Label	Unlabel+Label
Testing Accuracy	18.75%	59.37%	80.62%
Training Latency (h)	0	4.14	85.83 + 2.07

Table 3: Model performance of three different learning approaches. “Pre-trained” means directly applying the pre-trained model to the target subject. “Supervised” means learning from scratch with limited labeled data from the subject. “Semi-supervised” trains the models with both unlabeled and limited labeled data. The training latency is measured during the on-device model training on the ADMarker prototype.

4.1.2 *Performance of different learning approaches.* We then evaluate the performance of different traditional learning approaches to motivate the design of our federated learning architecture. The task is to classify 22 daily living activities related to Alzheimer’s Disease using audio, depth, and radar data. The testing data is collected from a subject over four weeks, with a total of 500 samples. There are 200 labeled training samples and 4,000 unlabeled training samples from the target subjects. The pre-trained model is trained using labeled data (3,728 samples) from another nine subjects.

Table 3 shows the model testing accuracy and on-device training latency of different training schemes. First, directly applying the pre-trained model to the new subject results in a low testing accuracy (i.e., only 18.75%), which shows that there is a huge domain gap among the data of different subjects. Second, when there is only limited labeled training data (the supervised approach), the model accuracy is still unsatisfactory, i.e., 59.37%. And the model accuracy can be improved by unsupervised multi-modal learning that leverages large amounts of unlabeled data from the subject (the semi-supervised approach). However, when learning from scratch, unsupervised model training with large amounts of unlabeled data will incur significant computing overhead on the edge device, i.e., about 85 hours.

4.2 Design Overview: A Three-Stage Federated Learning Architecture

Motivated by the case study, we propose a novel three-stage federated learning architecture that integrates a pre-trained model on the cloud and leverages both unlabeled and labeled data on nodes deployed in the subjects’ homes. As shown in Figure 4, at the first stage, we train a multi-modal model using the labeled data on the server. Such training data can leverage the public data sets that have already been made public. For instance, the data collected from this work will be made public and utilized for model pre-training in future deployments. Then, during the deployment, the nodes in the subjects’ homes will load the centrally pre-trained model, and

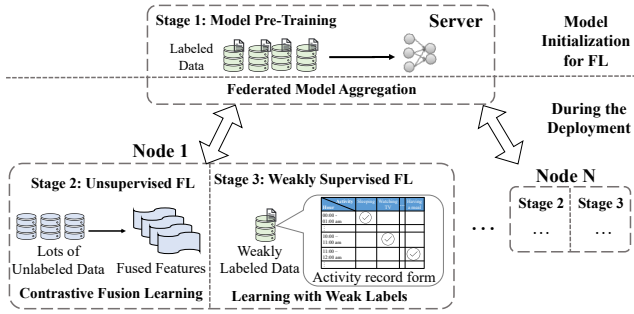


Figure 4: The three-stage federated learning architecture of ADMarker. Stage 1: Centralized model pre-training; Stage 2: Unsupervised multi-modal FL; Stage 3: Weakly supervised multi-modal FL.

improve the model performance on their own data through two-stage federated learning, i.e., unsupervised multi-modal FL and weakly supervised multi-modal FL, respectively.

The reasons for the three-stage training design are as follows. First, the model trained on the cloud needs to be retrained to adapt to the local data of each subject. Second, training the multi-modal network from scratch with noisy real-world data is an extremely challenging task in FL settings. The pre-trained model can reduce the computing overhead of online FL training. Third, there usually exists a very small amount of labeled data, as it is difficult to label multi-modal data in real-world settings. Therefore, the nodes perform unsupervised FL to leverage the large amounts of unlabeled multi-modal data, and weakly supervised FL based on limited weakly labeled data. The weak labels for supervised local training are provided by the participants (see Section 4.4). For example, marking the time of having lunch would automatically label the multi-modal data during lunch. In the following, we focus on the framework of unsupervised and supervised multi-modal federated learning.

4.3 Unsupervised Multi-Modal FL

In this stage, the nodes will download the pre-trained model from the server, and collaboratively train feature encoder networks of different data modalities (i.e., depth images, audio, and radar data) using the collected unlabeled sensor data during deployment. There are two main challenges during the unsupervised federated learning stage. First, the sensor modalities produce highly heterogeneous information about the same events/activities. For example, the audio features and radar data have significantly different dimensions and patterns, making it challenging to extract useful information. Second, the sensor modalities available on different nodes may vary due to the deployment constraints or runtime system dynamics. For example, some families may not be willing to have depth cameras installed in the bedroom, and the sensors may fail dynamically, e.g., due to power surges.

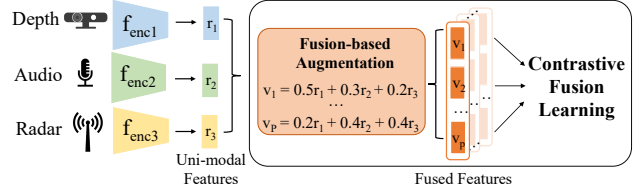


Figure 5: Contrastive fusion learning on nodes. Through contrastive learning on the extensively augmented fused features, the uni-modal feature encoders are trained to capture consistent information from unlabeled multi-modal data.

Therefore, the design of unsupervised multi-modal FL should adapt to different modality combinations.

To address these challenges, the nodes will run fusion-based contrastive learning that trains the feature encoders by exploring the consistent information of heterogeneous data modalities. The server will aggregate the feature encoders of nodes with heterogeneous data modalities through modality-wise federated averaging. Compared with traditional multi-modal FL approaches, the key advantage of this idea is that it is oblivious to differences of modalities on nodes.

Contrastive fusion learning on nodes. During local training, a fusion-based feature augmentation module [45] will extensively augment the uni-modal features (extracted by encoders of different modalities) to a group of fused features via weighted sum or concatenation. As shown in Figure 5, each augmented feature represents a different fusion combination of the sensor features and contains some subset of information in the original data sample. Let $s \in S \equiv \{1, 2, \dots, P \times N\}$ be the index of an arbitrary augmented feature, and let $p \in P(s)$ be the index of the other augmented features originating from the same source sample. The contrastive fusion loss can be defined as:

$$\mathcal{L}_{conf} = \sum_{s \in S} \frac{-1}{|P(s)|} \sum_{p \in P(s)} \log \frac{\exp(\mathbf{v}_s \cdot \mathbf{v}_p / \tau)}{\sum_{a \in S \setminus \{s\}} \exp(\mathbf{v}_s \cdot \mathbf{v}_a / \tau)}. \quad (1)$$

Here \mathbf{v}_s is the feature output of the fusion-based augmentation module, and the symbol \cdot denotes the inner product of feature vectors. Parameter $\tau \in \mathbb{R}^+$ represents the temperature used to adjust the impact of different samples [58]. Therefore, minimizing the contrastive fusion loss will force the fused features from the same multi-modal data sample (positive features, \mathbf{v}_s and \mathbf{v}_p) together, while pushing fused features from other data samples (negative features, \mathbf{v}_s and \mathbf{v}_a) apart. In this way, the feature encoders are trained to learn consistent information across modalities by maximizing the mutual information of features from different modalities.

Modality-wise federated average. In multi-modal FL systems, the nodes with different data modalities will have different model architectures. For example, the nodes with all data modalities will train models with three multi-modal

feature encoders, while the models of nodes with only depth and audio data will train models with two feature encoders. We propose a modality-wise federated average scheme to address the challenge of modality heterogeneity, where the server will collect and aggregate the encoder networks of the same modality with Fedavg [39]. As a result, the nodes with different data modalities can collaborate to improve the performance in unsupervised federated learning. We also apply this model aggregation scheme on the server during the weakly supervised multi-modal FL stage.

4.4 Weakly Supervised Multi-Modal FL

At the third stage, the nodes will perform weakly supervised multi-modal FL based on the model trained at the second stage. During the real-world deployment, the nodes can leverage weak labels provided by the participants or their caregivers for local model training. For example, marking the time of having lunch would automatically label the sensor data during the period. However, it would be challenging to associate the sparse and noisy labels with collected sensor data for supervised model training. Moreover, different subjects usually have highly heterogeneous and imbalanced data distributions, making it challenging for model aggregation in FL. For example, some activities such as “sitting” incur frequently while others like “writing” appear rarely.

Training with weak labels. ADMarker leverages sparse activity logs for weakly supervised training. Such logs can be obtained in several different ways. Many patients are routinely suggested by the doctors to keep a journal of activity logs through ADL scales [49]. Alternatively, the patients and/or their caregivers may be asked to keep an activity log for the purpose of user training during the initial phase of system deployment. Our results show that ADMarker achieves good performance even if activity logs are available for only several days (see Figure 12a). Moreover, only major daily routines like “sleeping”, “having a meal” (see Fig. 6(a)) are needed, which alleviates the burden of users.

To train the model with weak labels, we first need to map them to a series of fine-grained activity labels we are interested in (see Table 2), which requires sophisticated domain knowledge. For example, the weak label “Having a meal” corresponds to the fine-grained labels “eating” and “setting”, while “Household” includes the activities of “standing” and “walking”. Another challenge is to associate the mapped fine-grained labels with collected sensor data, because the mapping from weak to fine-grained labels does not include the order of the events. Therefore, during the weakly supervised training, we split the training data such that the data samples in the same batch are collected successively in the time order. Then, to improve the training performance, we shuffle the training samples in each batch to simulate different orders

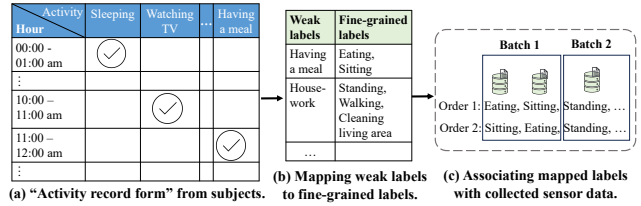


Figure 6: Training with weak labels. The “activity record form” provided by subjects is mapped to fine-grained labels and associated with collected data.

of the activities, and calculate the cross entropy loss with different label permutations for model training.

Local and global balancing on nodes. To address the challenge of local class imbalance, the nodes will perform both self and global balancing during model training. First, the nodes will use balanced cross-entropy loss [30] $\mathcal{L}_{balanceCE}$ to train the local model, which avoids the gradient dominance of the majority classes. In particular, the standard cross entropy loss will be reweighted with the number of samples in each class to down-weight the loss assigned to head classes. Moreover, as FL proceeds, the server-side global model more or less accumulates some knowledge on all classes [52]. Therefore, the aggregated global model will serve as the teacher model to guide the training of the local model using knowledge distillation [21] with the loss \mathcal{L}_{KD} . Therefore, the overall training loss of nodes during the weakly supervised FL stage is added by $\mathcal{L}_{balanceCE}$ and \mathcal{L}_{KD} .

5 UTILIZING DIGITAL BIOMARKERS FOR AD ANALYSIS

To evaluate the effectiveness of the detected biomarkers, we use a DNN for AD diagnosis, where the inputs are the features of the digital biomarkers and outputs are the predictions of diagnosis results. Then, the major challenge is how to quantify the digital biomarkers to generate effective features as the input of the disease diagnosis model. According to medical literature [18], we calculate the duration and frequency of the detected activities over the period of deployment as the features. However, due to the system dynamics (see Section 4.1.1), the total duration of the recorded sensor data may vary among different subjects. For example, most of the subjects will have four-week data, while some subjects only have one-week or two-week data due to sensor faults. Therefore, we further normalize the duration and frequency of detected activities with the period of the collected data.

Moreover, to further select more effective digital biomarkers, we use one-way Analysis of Variance (ANOVA) [55] to measure the correlations between each digital marker and the diagnosis results. Before applying ANOVA analysis to the data collected in our clinical deployment, we need to ensure that our data satisfies the following three conditions:

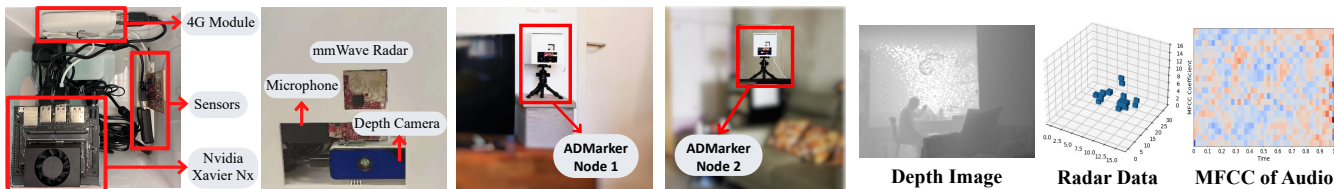


Figure 7: The ADMarker prototype. The hardware incorporates three sensor modalities (depth, mmWave radar, and audio) to detect multi-dimensional behavior biomarkers in home environments.

independence, normality, and equality. First, the selected features of each individual are independent of others, either in the same or different subject groups (NC, MCI, and AD). Second, we apply the Box-Cox data transform [51] to the selected features, ensuring that the transformed features satisfy the normal distributions. Third, we use the Levene’s test [14] to access the variances of each feature among the AD, MCI, and NC groups. The mean p-value (0.659) is larger than 0.05, which shows the equality of selected features.

6 SYSTEM IMPLEMENTATION

6.1 Hardware System

Figure 7 shows the overview of our ADMarker prototype. The hardware system incorporates three multi-modal sensors, an NVIDIA single-board edge computer, and a 4G cellular interface that communicates with the server.

6.1.1 Hardware choices. The goal of the hardware design is to capture lots of digital biomarkers in a privacy-preserving manner while ensuring durability and scalability of the system. First, we choose three sensor modalities: a depth camera, a mmWave radar, and a microphone, which collectively capture a wide range of biomarkers while preserving the users’ privacy. In particular, the Time-of-Flight (ToF) depth camera cannot reveal sensitive personal information like faces; the mmWave radar can only detect the motions of the subjects; the ambient microphones run real-time algorithms to extract acoustic features without recording any raw acoustic data. Collectively, the three sensor modalities can detect various activities such as having meals, conversations, watching TV, etc. Second, we choose the NVIDIA Xavier NX [3] as the main compute unit as it incorporates powerful NVIDIA GPUs (384-core Volta) and CPUs (6-core @1.9GHZ) for on-device model training. Third, to improve the durability of the system, we choose the NVMe SSD rather than the conventional portable HDD or SSD as the external data storage unit. The reason is that they have a relatively lower read/write speed (about 100MB/s), poor reliability (vulnerable to vibration and power failure), and a larger size/weight, which is unsuitable for long-term operation and mass deployment.

6.1.2 Layout design. The design of our hardware system comprises a number of components (e.g., sensors, accessories,

and cables) in a single box, which increases the difficulty of box assembly and heat dissipation. We carefully optimize the cabling and group similar components within the same shelf, making the box compact and lightweight. The size of the hardware box is about 20cm x 20cm x 20cm. Moreover, the sensing coverage of the sensors is limited, e.g., with the range of 0.35m-4.4m and a field-of-view (FOV) of 69°(H) x 51°(V) for the depth camera. In order to capture the main area of a living room and reduce the domain gap of different subjects’ data, we add a tripod at the bottom of the box to adjust the height and angle of the box.

6.2 Software System

We now present the design of several major functions to improve the stability and scalability of the software system.

6.2.1 Long-term multi-modal sensor data recording and pre-processing. First, ADMarker needs to collect and store the data of multiple sensors continuously for up to months, which requires a large storage space and incurs significant power consumption. In particular, we set the sampling rates of the depth camera, mmWave radar, and microphone as 15 Hz, 20 Hz, and 44,100 Hz, respectively, which will result in around 4TB data during a four-week deployment. To address this challenge, we save the depth data in an 8-bit format and compress the images into videos with OpenCV MJPG [4], bringing about a 75% reduction in data volume without significantly sacrificing the data quality. Second, the sensors may stop data recording occasionally, e.g., due to power surges or unstable sensor connections. We use the *systemd* service [5] of Linux to restart the sensors in case of sensor failures. Finally, to train the multi-modal models, the recorded sensor data is split into 2-second samples, and then converted into a fixed dimension [16,112,112], [20,2,16,32,16], and [20,87] for depth (cropped images), radar (voxels), and audio (Mel-frequency cepstral coefficients), respectively.

6.2.2 Improving training and inference efficiency. During online FL, a major challenge of continuous training and inference with all collected sensor data is the significant delay. For example, Table 3 shows that unsupervised FL with 4,000 samples (i.e., data collected in about 2.2 hours) will incur a training delay of 85 hours (3-4 days). This will not only

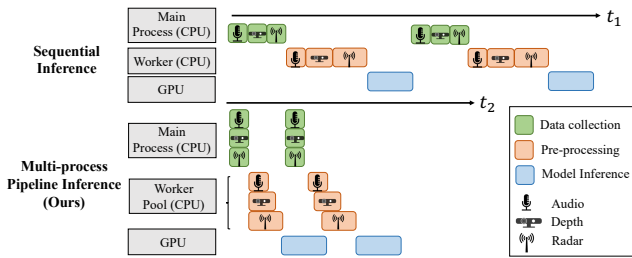


Figure 8: Illustration of our multi-process pipeline inference and conventional sequential inference scheme.

increase the data storage requirement on the device, but also affect the model accuracy due to the delayed updating of collected data during model training. Therefore, we propose two approaches to improve training and inference efficiency.

First, we apply the following online data selection strategies to reduce the model training delay while maintaining the effectiveness of AD symptom monitoring. Basically, the sensors will only collect data during a 12-hour period (i.e., 7:00-19:00) that contains fundamental daily activities, such as having meals, house-holding, etc. Moreover, rather than saving all recorded data, we evenly sample the data over time and only choose 1% of the data for model training. The reason is that most activities of interest, such as sitting, walking, or standing, last for a relatively long time (e.g., several minutes). Finally, we use Yolov5 [6] to detect humans in the depth images and delete the data samples without humans.

To reduce the on-device inference latency, we design a multi-task scheduling scheme for accelerating the pipeline in end-to-end multi-modal inference, including multi-sensor data collection, data pre-processing, and model inference. As shown in Figure 8, ADMarker will run the three major tasks in parallel instead of processing them sequentially. For example, during the inference of previous data frames on GPU, the tasks of recording and pre-processing the incoming data frames are scheduled to utilize the spare resources on CPUs. Moreover, ADMarker maintains a pool of processes to handle the data pre-processing tasks of three different modalities in parallel, further reducing the inference latency. As a result, ADMarker can detect biomarkers in real-time, e.g., 9.45 frames per second (of depth data) in the end-to-end multi-modal inference.

6.2.3 Private and stable communication networks. To enable federated learning, the system should have highly stable and secure Internet connectivity to the server. However, the home WiFi or Ethernet connection of users should not be used due to privacy and cost concerns. Therefore, the ADMarker nodes are incorporated with a cellular interface to communicate with the server using 4G LTE through a Virtual Private Network (VPN). Moreover, to reduce the communication delay, we dynamically select the optimal frequency band on each node according to the runtime demand of FL, e.g.,

Group	AD	MCI	NC
No. of subjects	31 (M/F:10/21)	30 (M/F:18/12)	30 (M/F:20/10)
Age (Mean±STD)	79.53±7.11	78.14±5.73	70.66±6.94
Living Mode (A/W-F/W-C)	2/25/4	2/27/1	6/24/0
Education Years (Mean±STD)	6.16±3.82	5.79±3.70	10.59±4.10
MoCA Score (Mean±STD)	11.75±6.38	19.50±6.53	25.07±4.41

Table 4: Demographic characteristics of enrolled elderly subjects (N = 91). A: Alone; W-F: With Family; W-C: With Caregiver. MoCA: Montreal Cognitive Assessment [43].

B3 (1800Mhz, 21Mbps) when uploading models to the server and B40 (2300Mhz, 20Mbps) when downloading models.

7 CLINICAL DEPLOYMENT

A total of 91 elderly subjects (43 females and 48 males), aged between 61 and 93 years old, have participated in our clinical study¹. As shown in Table 4, the participants were from three groups: 31 with Alzheimer’s Disease, 30 with mild cognitive impairment (MCI), and 30 are cognitively normal. The ADMarker node will be installed at the height of 1.5m-1.8m in the living room of the subject’s home for four weeks, as shown in Figure 7b. The installation process typically takes about ten minutes per home. The subjects and their caregivers were asked to fill in an “activity record form” by ticking the relevant daily activities, which served as the weak labels for behavior analysis (see Section 4.4).

Diagnosis of the subjects. Before the study, each elderly subject underwent a screening test (i.e., Montreal Cognitive Assessment [43], MoCA) to generate a cognitive score. A low MoCA score indicates the risk of cognitive impairment. The subjects then received physical examinations and face-to-face consultations with a neuropsychologist if they: (1) have no medical record of AD diagnosis but receive low cognitive scores in the screening test; (2) already have a medical record of AD diagnosis before, but their cognitive scores are obviously inconsistent with the medical records. Moreover, patients with AD and MCI who have not received an MRI test within one year are suggested to do a free MRI test, while the MRI test is voluntary for cognitively normal subjects. Then, the neuropsychologist will give the final diagnosis results of the enrolled subjects by combining the results of the face-to-face interview and MRI scan.

8 EVALUATION

8.1 Methodology

Experiment settings. Our evaluation is based on the clinical study of total 91 subjects. The ADMarker systems deployed in these subjects’ homes collected a total of 61,152 hours of multi-modal sensor data, with a total size of over

¹All the data collection was approved by IRB and the Clinical Research Ethics Committee of the authors’ institution.

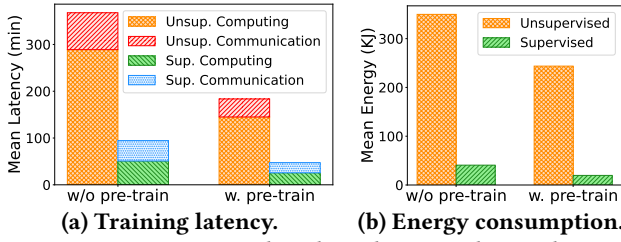


Figure 9: System overhead with or without the pre-trained model. “Unsup. Computing” denotes the computing time of nodes in unsupervised FL.

91TB. Among these, the data of 31 subjects is used for model pre-training, and 60 deployed nodes run the unsupervised and weakly supervised federated learning algorithms continuously for four weeks. To evaluate the performance of AD diagnosis using the detected digital biomarkers, we adopt 3-fold cross-validation using the data of 69 subjects (22 AD, 25 MCI, 22 NC), because the remaining 22 subjects either have less than one week of valid sensor data or limited labeled data that contains humans (e.g., tens of samples). We use the software packages *jetson-stats* from JetPack 4.6.1 [7] to record the power, memory/CPU/GPU usage and temperature of the hardware system, and use *speedtest-cli* [8] to measure the network bandwidth and latency.

Configurations of models. We use a CNN to extract deep features and a two-layer RNN to capture the time-series properties in the feature encoders, and use two dense layers for the classifier. Here 2D-CNN is used for audio MFCC features, and 3D-CNN is used for depth and radar data. The learning rate and batch size are 0.01 and 16 for unsupervised FL, and 0.001 and 16 for supervised FL. We use the data collected in the first and last weeks for model training and evaluation, respectively.

Data annotation As a long-term autonomous monitoring system, ADMarker is expected to rely on as few manual annotations as possible. We use the “activity record form” (see Section 4.4) provided by the subjects to generate the weak labels for weakly supervised FL. Moreover, the multi-modal data collected by the system are synchronized using the system clock and annotated using depth videos by a professional data labeling company. The manually labeled data is used as ground truth for evaluating the performance of our system and helps to understand the performance of leveraging weak labels.

8.2 System Overhead

In this section, we evaluate the system overhead of ADMarker during federated learning in the presence of various system dynamics (see Section 4.1.1). For example, during the 4-week

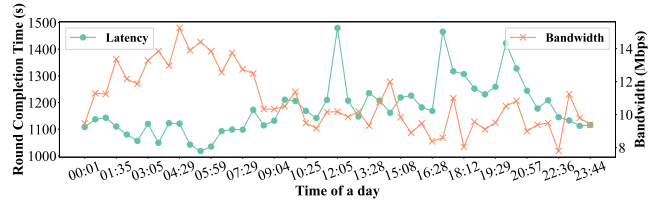


Figure 10: Round completion time of FL and mean bandwidth in a 24-hour operation.

deployment, the sensors may stop data recording occasionally due to power surges or unstable sensor connections. The bandwidth of nodes also fluctuates over time.

Figure 9 compares the mean training latency and energy consumption with or without centralized model pre-training in online FL. Here, the numbers of training samples in unsupervised and supervised FL are 300 and 100, respectively. When the models of nodes are initialized with the pre-trained model, the system overhead of both unsupervised and supervised FL is significantly reduced. For example, in unsupervised FL, the overall training latency and the energy consumption are reduced by 184.3min and 106KJ, respectively, since the models converge faster than training from scratch. Moreover, the system overhead of supervised FL is much smaller than unsupervised FL, because the feature encoder networks are already trained with large amounts of unlabeled multi-modal data in unsupervised FL.

Figure 10 plots the variation of round completion time of FL and mean downlink bandwidth of nodes at different time of the day. The round completion time denotes the latency of finishing one global round of unsupervised FL (i.e., computing time for local training plus communication time). Generally, the training latency of one FL round at nighttime is shorter than at daytime (by about 14%), because of a better 4G LTE network connectivity. Moreover, the latency increases significantly at around 12:00, 17:00, and 19:00, which is probably caused by the increased network traffic from smartphone users during/after mealtimes. Therefore, the nodes in ADMarker could run federated learning at nighttime to reduce the overall training latency. We also note that the network congestion or node disconnectivity will not affect the accuracy of biomarker detection.

8.3 Accuracy of Biomarker Detection

8.3.1 Overview of the subjects’ data. We first show the overall characteristics of data collected by ADMarker during the four weeks of real-world deployment. First, Figure 11 shows examples of the class distribution across nine subjects for daily living activities and basic body movements, respectively. We can observe obvious class imbalance in different subjects’ local data. Moreover, the class distributions of different subjects are highly non-i.i.d. Second, Figure 12a shows that there is only limited labeled sensor data during

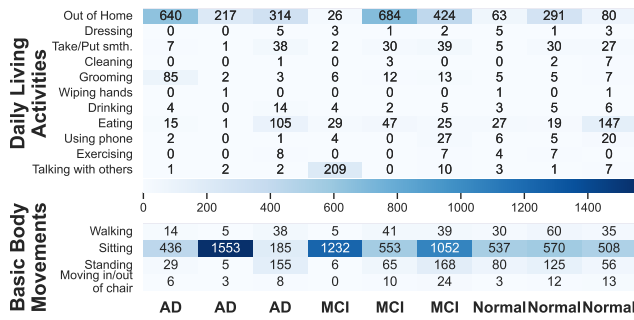


Figure 11: Examples of activity distribution across nine subjects. The numbers denote the amount of data samples of the activities over four weeks.

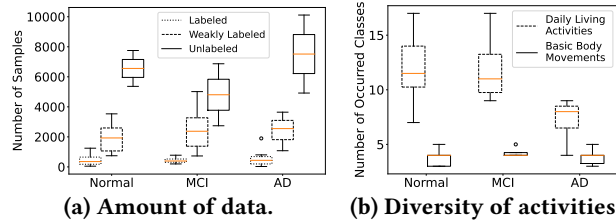


Figure 12: Data summary of different subject groups.

real-world deployment, due to the significant overhead and cost of data annotation. For example, the average amount of labeled data is less than 10% of unlabeled data. However, the amount of data with weak labels (see Section 4.4) is much larger than manually annotated data, which can be leveraged to effectively train the models. Finally, Figure 12b presents the number of occurred activities during the deployment. In daily living activities, cognitively normal and MCI subjects exhibit more diverse activities than AD subjects, which shows the decline in cognitive and functional ability during the progression of AD [33].

8.3.2 Performance of biomarker detection. Figure 13 shows the accuracy of biomarker detection under different settings.

Performance at different stages of FL. Figure 13(a) shows the accuracy at different stages of federated learning. First, directly applying the pre-trained model has a very low detection accuracy on the participants during the deployment due to the large domain gap, e.g., with a mean accuracy of 56.37%. Second, although the model accuracy after unsupervised FL (Stage 2 of ADMarker) is still low since the classifier layers are not trained, the feature encoders trained using large amounts of unlabeled data can significantly improve the accuracy performance at Stage 3. Finally, full-fledged ADMarker with a three-stage FL design can improve the model accuracy by combining the unlabeled and labeled data, e.g., 89.56% and 93.81% mean accuracy with weak and annotated labels, respectively.

Performance on different subjects. Figure 13(b) shows the accuracy of biomarker detection on different subject

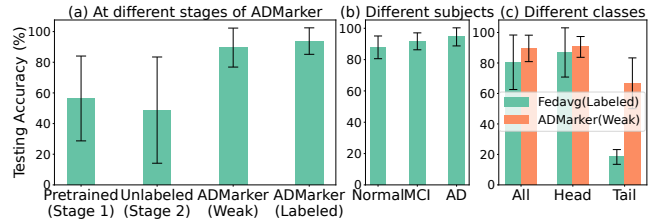


Figure 13: Accuracy of biomarker detection at different stages, on different subject groups and activity classes.

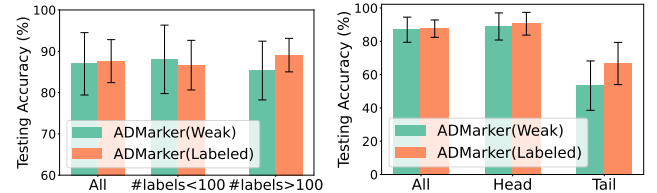


Figure 14: Understanding the weak labels by comparing with the performance using manually labeled data.

groups, which varies among the three subject groups. In particular, the mean accuracy is over 94.51% for AD subjects, while 87.83% and 91.67% for cognitively normal and MCI subjects, respectively. The reason is that the cognitively normal and MCI subjects generally exhibit significantly more diverse behaviors in daily living (see Figure 12b), increasing the difficulty of detection.

Dealing with class imbalance. Figure 13(c) compares the performance of Fedavg with manually labeled data and ADMarker with weak labels on detecting different classes of activities. The models are initialized with weights trained at the second stage of ADMarker. We define the behaviors with the most and least four data samples as the head classes (i.e., walking, sitting, standing, and eating) and tail classes (i.e., cleaning the living area, grooming, wiping hands, and exercising), respectively. Compared with Fedavg, the overall accuracy (all classes) is improved by ~9%. However, Fedavg exhibits a very bad accuracy in detecting the tail classes, with ~18.33% on average. Our approach can improve the performance on tail classes by ~48.33% compared with Fedavg.

8.3.3 Understanding the weak labels. We further study the effectiveness of learning with weak labels in Section 4.4 by comparing the performance with manually annotated data. To avoid the impact of different subject groups, the results are based on the data of cognitively normal subjects.

With different amounts of annotated data. Figure 14a compares the performance of two approaches among subjects with different amounts of annotated data. Although the weak labels provided by the subjects are usually noisy and sparse, the amount of associated weakly labeled data is usually larger than manually annotated data (see Figure 12a). Therefore, when the subjects have very limited data (#

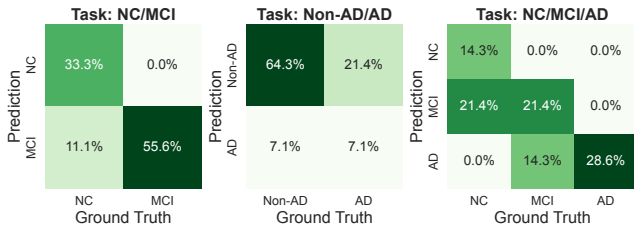


Figure 15: The confusion matrix of utilizing the digital biomarkers for different AD diagnosis tasks.

of labels < 100), ADMarker with weak labels even performs better than with annotated labels, e.g., by 1.41% improvement in mean accuracy. However, when the subjects have enough labeled data (# of labels < 100), ADMarker with annotated data will have a better accuracy performance.

On different classes. We then compare the performance of two approaches on different classes, where the head and tail classes are defined the same as Section 8.3.2. Compared with ADMarker with annotated labels, the performance with weak labels is very close on the head classes, while worse on the tail classes. The reason is that the weak labels provided by the subjects are more reliable on “persistent” activities like walking, sitting, and eating, while noisy on dynamic activities like cleaning the living area, wiping hands, and exercising. Therefore, the performance of ADMarker with weak labels can be further improved if we combine only a limited amount of annotated labels on the tail classes.

8.4 Interpretation of Detected Biomarkers

8.4.1 Utilizing the biomarkers for AD diagnosis. Figure 15 shows the effectiveness of utilizing the detected digital biomarkers for three diagnostic tasks (i.e., normal/MCI, non-AD/AD, and normal/MCI/AD). These tasks are clinically important and are consistent with the current practice of AD diagnosis [32, 38]. First, ADMarker achieves about 88.9% accuracy (33.3%+55.6%) in classifying MCI and cognitively normal subjects, meaning that ADMarker is able to identify people at early stage of AD. Second, the accuracy of non-AD/AD and normal/MCI/AD is 71.4% and 64.3%, respectively, which shows that identifying MCI from AD subjects is very difficult for subjects with various demographic and medical characteristics. Nevertheless, the results are better than the state-of-the-art studies based on a single digital biomarker. For example, Tatc [29] identifies MCI with only 42.3% accuracy, and ADReSS [35] achieves 60.8% for detecting AD.

8.4.2 Advantages of leveraging multiple biomarkers. Figure 16a compares the accuracy of identifying normal/MCI/AD, with vision-based biomarkers (e.g., walking, standing) using depth and radar data, audio-based biomarkers (e.g., talking) that can be captured with microphones, and all biomarkers (e.g., eating, phone call) that need a combination of all three

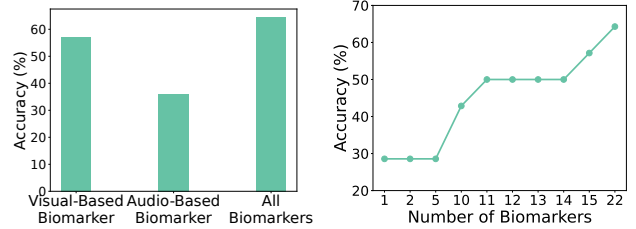


Figure 16: Impact of leveraging multiple biomarkers.

sensors. We observe that the diagnosis accuracy with only a single sensor modality is relatively low, e.g., 57.1% and 35.7% for vision and audio-based biomarkers, respectively. When multiple sensor modalities are used, the diagnosis accuracy has more than about 30% improvement over single modality-based biomarkers. Figure 16b shows the diagnosis accuracy with different numbers of biomarkers, where the biomarkers are sequentially added with the order of class index in Table 2. The results show that more than a few biomarkers are needed for accurate AD diagnosis, which demonstrates the significance of integrating multiple sensors for detecting multidimensional biomarkers in ADMarker.

8.4.3 Correlation analysis with the diagnosis results. Our results not only identify AD, but also shed light on system design, e.g., what digital biomarkers should be monitored more accurately, which reduces the system’s cost and improves the detection accuracy. Specifically, we analyze the correlation between each biomarker and the three diagnostic tasks with ANOVA [55]. We name those biomarkers with a p-value less than 0.05 as *critical digital biomarkers*, as they are strongly associated with the diagnostic tasks. First, the critical digital biomarkers for different diagnostic tasks are different. For example, phone calls, walking, and standing have a strong correlation in differentiating AD/non-AD, yet are not that useful in identifying normal and MCI. Moreover, it is extremely hard to differentiate cognitively normal subjects and MCI, as only “sitting” is strongly correlated with this diagnosis task. This also shows that MCI and cognitively normal subjects exhibit similar activity behaviors.

In addition, we evaluate the impact of gender and age on diagnosis accuracy using the detected digital biomarkers. The results show that the diagnosis accuracy is similar among males (80.55%) and females (81.82%). Moreover, the digital biomarkers are more effective for the subjects aged 60-70 (88.89%) and 80-90 (89.47%) years old, compared with subjects aged 70-80 years old (84.38%). We believe these results provide insights into further investigation in AD research.

9 CONCLUSION AND DISCUSSION

We propose ADMarker, the first end-to-end system that integrates multi-modal sensors and new federated learning algorithms for detecting multidimensional AD digital biomarkers in natural living environments. This study provides key insights into the development of clinically proven digital biomarkers for early AD diagnosis and intervention.

Here we discuss some limitations of our design and future work. First, due to various human factors, the weak labels extracted from the activity logs for online supervised FL are usually very sparse and limited. In the future, we will develop new approaches that require fewer weak labels during the deployment, e.g., by associating the weak and manually annotated labels during model pre-training on the cloud. The design of ADMarker can also leverage pseudo-labels automatically generated by running image classification algorithms on high-quality depth data [60, 61]. Moreover, we will launch a larger-scale clinical study with an improved hardware design of ADMarker. We will also investigate personalized intervention strategies for different individuals based on the multi-dimensional digital biomarkers identified in this work.

REFERENCES

- [1] 2021. World Alzheimer Report 2021: Journey through the diagnosis of dementia. <https://www.alzint.org/resource/world-alzheimer-report-2021/>. (2021).
- [2] 2022. ALZHEIMER'S DIGITAL BIOMARKERS. <https://www.alzdiscovery.org/research-and-grants/funding-opportunities/diagnostics-accelerator-digital-biomarkers-program>. (2022).
- [3] 2022. NVIDIA Xavier NX. <https://www.nvidia.com/en-us/autonomous-machines/embedded-systems/jetson-xavier-nx/>. (2022).
- [4] 2022. Opencv MJPG. https://docs.opencv.org/4.x/dd/d43/tutorial_py_video_display.html. (2022).
- [5] 2022. Systemd. <https://en.wikipedia.org/wiki/Systemd>. (2022).
- [6] 2022. Yolov5. (2022). https://pytorch.org/hub/ultralytics_yolov5/.
- [7] 2023. jetson-stats. (2023). https://github.com/rbonghi/jetson_stats.
- [8] 2023. speedtest-cli. (2023). <https://pypi.org/project/speedtest-cli/>.
- [9] Ane Alberdi, Alyssa Weakley, Maureen Schmitter-Edgecombe, Diane J Cook, Asier Aztiria, Adrian Basarab, and Maitane Barrenechea. 2018. Smart home-based prediction of multidomain symptoms related to Alzheimer's disease. *IEEE journal of biomedical and health informatics* 22, 6 (2018), 1720–1731.
- [10] Manuela Altieri, Federica Garramone, and Gabriella Santangelo. 2021. Functional autonomy in dementia of the Alzheimer's type, mild cognitive impairment, and healthy aging: a meta-analysis. *Neurological Sciences* 42 (2021), 1773–1783.
- [11] Asuna Arai, Amartuvshin Khaltar, Takashi Ozaki, and Yuriko Katsumata. 2021. Influence of social interaction on behavioral and psychological symptoms of dementia over 1 year among long-term care facility residents. *Geriatric nursing* 42, 2 (2021), 509–516.
- [12] Sayeh Bayat, Ganesh M Babulal, Suzanne E Schindler, Anne M Fagan, John C Morris, Alex Mihailidis, and Catherine M Roe. 2021. GPS driving: a digital biomarker for preclinical Alzheimer disease. *Alzheimer's Research & Therapy* 13, 1 (2021), 1–9.
- [13] Lisa F Berkman, Thomas Glass, Ian Brissette, and Teresa E Seeman. 2000. From social integration to health: Durkheim in the new millennium. *Social science & medicine* 51, 6 (2000), 843–857.
- [14] Morton B Brown and Alan B Forsythe. 1974. Robust tests for the equality of variances. *Journal of the American statistical association* 69, 346 (1974), 364–367.
- [15] Nam Bui, Anh Nguyen, Phuc Nguyen, Hoang Truong, Ashwin Ashok, Thang Dinh, Robin Deterding, and Tam Vu. 2017. PhO2: Smartphone Based Blood Oxygen Level Measurement Systems Using Near-IR and RED Wave-Guided Light. In *Proceedings of the 15th ACM Conference on Embedded Network Sensor Systems (SenSys '17)*. Association for Computing Machinery, New York, NY, USA, Article 26, 14 pages. <https://doi.org/10.1145/3131672.3131696>
- [16] Xiangmao Chang, Cheng Peng, Guoliang Xing, Tian Hao, and Gang Zhou. 2020. ISleep: A Smartphone System for Unobtrusive Sleep Quality Monitoring. *ACM Trans. Sen. Netw.* 16, 3, Article 27 (jul 2020), 32 pages. <https://doi.org/10.1145/3392049>
- [17] Richard Chen, Filip Jankovic, Nikki Marinsek, Luca Foschini, Lampros Kourtis, Alessio Signorini, Melissa Pugh, Jie Shen, Roy Yaari, Vera Maljkovic, et al. 2019. Developing measures of cognitive impairment in the real world from consumer-grade multimodal sensor streams. In *Proceedings of the 25th ACM SIGKDD international conference on knowledge discovery & data mining*. 2145–2155.
- [18] Prafulla Nath Dawadi, Diane Joyce Cook, and Maureen Schmitter-Edgecombe. 2015. Automated cognitive health assessment from smart home-based behavior data. *IEEE journal of biomedical and health informatics* 20, 4 (2015), 1188–1194.
- [19] SF Doris, Timothy Kwok, Jacky Choy, and David J Kavanagh. 2016. Measuring the expressed emotion in Chinese family caregivers of persons with dementia: Validation of a Chinese version of the Family Attitude Scale. *International journal of nursing studies* 55 (2016), 50–59.
- [20] Kirsten M Fiest, Nathalie Jette, Jodie I Roberts, Colleen J Maxwell, Eric E Smith, Sandra E Black, Laura Blaikie, Adrienne Cohen, Lundy Day, Jayna Holroyd-Leduc, et al. 2016. The prevalence and incidence of dementia: a systematic review and meta-analysis. *Canadian Journal of Neurological Sciences* 43, S1 (2016), S3–S50.
- [21] Jianping Gou, Baosheng Yu, Stephen J Maybank, and Dacheng Tao. 2021. Knowledge distillation: A survey. *International Journal of Computer Vision* 129 (2021), 1789–1819.
- [22] Guoliang Xing. 2022. Machine Learning Technologies for Advancing Digital Biomarkers for Alzheimer's Disease, Alzheimer's Drug Discovery Foundation. <https://www.alzdiscovery.org/research-and-grants/portfolio-details/21130887>. (2022).
- [23] Margrét Gústafsdóttir. 2015. Is watching television a realistic leisure option for people with dementia. *Dementia and Geriatric Cognitive Disorders Extra* 5, 1 (2015), 116–122.
- [24] Robert Istepanian, Swamy Laxminarayan, and Constantinos S Pattichis. 2007. *M-health: Emerging mobile health systems*. Springer Science & Business Media.
- [25] Wenjun Jiang, Chenglin Miao, Fenglong Ma, Shuochao Yao, Yaqing Wang, Ye Yuan, Hongfei Xue, Chen Song, Xin Ma, Dimitrios Koutsonikolas, et al. 2018. Towards environment independent device free human activity recognition. In *Proceedings of the 24th Annual International Conference on Mobile Computing and Networking*. 289–304.
- [26] Jakub Konečný, H Brendan McMahan, Daniel Ramage, and Peter Richtárik. 2016. Federated optimization: Distributed machine learning for on-device intelligence. (2016). arXiv:1610.02527
- [27] Lampros C Kourtis, Oliver B Regele, Justin M Wright, and Graham B Jones. 2019. Digital biomarkers for Alzheimer's disease: the mobile/wearable devices opportunity. *NPJ digital medicine* 2, 1 (2019), 1–9.

- [28] Huining Li, Huan Chen, Chenhan Xu, Zhengxiong Li, Hanbin Zhang, Xiaoye Qian, Dongmei Li, Ming-chun Huang, and Wenyao Xu. 2023. NeuralGait: Assessing Brain Health Using Your Smartphone. *Proc. ACM Interact. Mob. Wearable Ubiquitous Technol.* 6, 4, Article 169 (jan 2023), 28 pages. <https://doi.org/10.1145/3569476>
- [29] Jia Li, Yu Rong, Helen Meng, Zhihui Lu, Timothy Kwok, and Hong Cheng. 2018. TATC: predicting Alzheimer’s disease with actigraphy data. In *Proceedings of the 24th ACM SIGKDD International Conference on Knowledge Discovery & Data Mining*. 509–518.
- [30] Tsung-Yi Lin, Priya Goyal, Ross Girshick, Kaiming He, and Piotr Dollár. 2017. Focal loss for dense object detection. In *Proceedings of the IEEE international conference on computer vision*. 2980–2988.
- [31] Xu-Ying Liu, Jianxin Wu, and Zhi-Hua Zhou. 2008. Exploratory under-sampling for class-imbalance learning. *IEEE Transactions on Systems, Man, and Cybernetics, Part B (Cybernetics)* 39, 2 (2008), 539–550.
- [32] Gill Livingston, Jonathan Huntley, Andrew Sommerlad, David Ames, Clive Ballard, Sube Banerjee, Carol Brayne, Alistair Burns, Jiska Cohen-Mansfield, Claudia Cooper, et al. 2020. Dementia prevention, intervention, and care: 2020 report of the Lancet Commission. *The Lancet* 396, 10248 (2020), 413–446.
- [33] Gill Livingston, Andrew Sommerlad, Vasiliki Orgeta, Sergi G Costafreda, Jonathan Huntley, David Ames, Clive Ballard, Sube Banerjee, Alistair Burns, Jiska Cohen-Mansfield, et al. 2017. Dementia prevention, intervention, and care. *The Lancet* 390, 10113 (2017), 2673–2734.
- [34] Hong Lu, Denise Frauendorfer, Mashfiqui Rabbi, Marianne Schmid Mast, Gokul T. Chittaranjan, Andrew T. Campbell, Daniel Gatica-Perez, and Tanzeem Choudhury. 2012. StressSense: Detecting Stress in Unconstrained Acoustic Environments Using Smartphones. In *Proceedings of the 2012 ACM Conference on Ubiquitous Computing (UbiComp ’12)*. Association for Computing Machinery, New York, NY, USA, 351–360. <https://doi.org/10.1145/2370216.2370270>
- [35] Saturnino Luz, Fasih Haider, Sofia de la Fuente, Davida Fromm, and Brian MacWhinney. 2020. Alzheimer’s Dementia Recognition through Spontaneous Speech: The ADReSS Challenge. In *Interspeech 2020*. ISCA, 2172–2176.
- [36] P Marique, F Peeters, K Herholz, D Perani, V Holthoff, E Kalbe, D Anichisi, S Adam, F Collette, G Garraux, et al. 2005. Cerebral metabolic correlates of four dementia scales in Alzheimer’s disease. *Journal of neurology* 252, 3 (2005), 283–290.
- [37] Gad A Marshall, Lynn A Fairbanks, Sibel Tekin, Harry V Vinters, and Jeffrey L Cummings. 2006. Neuropathologic correlates of activities of daily living in Alzheimer disease. *Alzheimer Disease & Associated Disorders* 20, 1 (2006), 56–59.
- [38] Gad A Marshall, Dorene M Rentz, Meghan T Frey, Joseph J Locascio, Keith A Johnson, Reisa A Sperling, and Alzheimer’s Disease Neuroimaging Initiative. 2011. Executive function and instrumental activities of daily living in mild cognitive impairment and Alzheimer’s disease. *Alzheimer’s & Dementia* 7, 3 (2011), 300–308.
- [39] H Brendan McMahan, Eider Moore, Daniel Ramage, Seth Hampson, et al. 2016. Communication-efficient learning of deep networks from decentralized data. *arXiv preprint arXiv:1602.05629* (2016).
- [40] Patrick McNamara, Loraine K Obler, Rhoda Au, Raymon Durso, and Martin L Albert. 1992. Speech monitoring skills in Alzheimer’s disease, Parkinson’s disease, and normal aging. *Brain and language* 42, 1 (1992), 38–51.
- [41] D Miu, SL Szeto, YF Mak, et al. 2008. A randomised controlled trial on the effect of exercise on physical, cognitive and affective function in dementia subjects. *Asian J Gerontol Geriatr* 3, 1 (2008), 8–16.
- [42] Manuel Montero-Odasso, Joe Verghese, Olivier Beauchet, and Jeffrey M Hausdorff. 2012. Gait and cognition: a complementary approach to understanding brain function and the risk of falling. *Journal of the American Geriatrics Society* 60, 11 (2012), 2127–2136.
- [43] Ziad S Nasreddine, Natalie A Phillips, Valérie Bédirian, Simon Charbonneau, Victor Whitehead, Isabelle Collin, Jeffrey L Cummings, and Howard Chertkow. 2005. The Montreal Cognitive Assessment, MoCA: a brief screening tool for mild cognitive impairment. *Journal of the American Geriatrics Society* 53, 4 (2005), 695–699.
- [44] Shamila Nasreen, Julian Hough, Matthew Purver, et al. 2021. Detecting Alzheimer’s Disease using Interactional and Acoustic features from Spontaneous Speech. *Interspeech*.
- [45] Xiaomin Ouyang, Xian Shuai, Jiayu Zhou, Ivy Wang Shi, Zhiyuan Xie, Guoliang Xing, and Jianwei Huang. 2022. Cosmo: contrastive fusion learning with small data for multimodal human activity recognition. In *Proceedings of the 28th Annual International Conference on Mobile Computing And Networking*. 324–337.
- [46] Xiaomin Ouyang, Zhiyuan Xie, Heming Fu, Sitong Cheng, Li Pan, Neiben Ling, Guoliang Xing, Jiayu Zhou, and Jianwei Huang. 2023. Harmony: Heterogeneous Multi-Modal Federated Learning through Disentangled Model Training. In *Proceedings of the 21st Annual International Conference on Mobile Systems, Applications and Services*. 530–543.
- [47] Xiaomin Ouyang, Zhiyuan Xie, Jiayu Zhou, Jianwei Huang, and Guoliang Xing. 2021. Clusterfl: a similarity-aware federated learning system for human activity recognition. In *Proceedings of the 19th Annual International Conference on Mobile Systems, Applications, and Services*. 54–66.
- [48] Xiaomin Ouyang, Zhiyuan Xie, Jiayu Zhou, Guoliang Xing, and Jianwei Huang. 2022. ClusterFL: A Clustering-based Federated Learning System for Human Activity Recognition. *ACM Transactions on Sensor Networks* 19, 1 (2022), 1–32.
- [49] Marian B Patterson, James L Mack, Marcia M Neundorfer, Richard J Martin, Kathleen A Smyth, and Peter J Whitehouse. 1992. Assessment of functional ability in Alzheimer disease: a review and a preliminary report on the Cleveland Scale for Activities of Daily Living. *Alzheimer Disease & Associated Disorders* 6, 3 (1992), 145–163.
- [50] Catherine Reed, Mark Belger, Bruno Vellas, Jeffrey Scott Andrews, Josep M Argimon, Giuseppe Bruno, Richard Dodel, Roy W Jones, Anders Wimo, and Josep Maria Haro. 2016. Identifying factors of activities of daily living important for cost and caregiver outcomes in Alzheimer’s disease. *International psychogeriatrics* 28, 2 (2016), 247–259.
- [51] Remi M Sakia. 1992. The Box-Cox transformation technique: a review. *Journal of the Royal Statistical Society Series D: The Statistician* 41, 2 (1992), 169–178.
- [52] Xian Shuai, Yulin Shen, Siyang Jiang, Zhihe Zhao, Zhenyu Yan, and Guoliang Xing. 2022. BalanceFL: Addressing class imbalance in long-tail federated learning. In *2022 21st ACM/IEEE International Conference on Information Processing in Sensor Networks (IPSN)*. IEEE, 271–284.
- [53] Xian Shuai, Yulin Shen, Yi Tang, Shuyao Shi, Luping Ji, and Guoliang Xing. 2021. millieye: A lightweight mmwave radar and camera fusion system for robust object detection. In *Proceedings of the International Conference on Internet-of-Things Design and Implementation*. 145–157.
- [54] Bruno MC Silva, Joel JPC Rodrigues, Isabel de la Torre Díez, Miguel López-Coronado, and Kashif Saleem. 2015. Mobile-health: A review of current state in 2015. *Journal of biomedical informatics* 56 (2015), 265–272.
- [55] Lars St, Svante Wold, et al. 1989. Analysis of variance (ANOVA). *Chemometrics and intelligent laboratory systems* 6, 4 (1989), 259–272.
- [56] Allan Stisen, Henrik Blunck, Sourav Bhattacharya, Thor Siiger Prentow, Mikkel Baun Kjærgaard, Anind Dey, Tobias Sonne, and Mads Møller Jensen. 2015. Smart devices are different: Assessing and mitigating mobile sensing heterogeneities for activity recognition. In *Proceedings of the 13th ACM conference on embedded networked sensor systems*. 127–140.

- [57] Sibel Tekin, Lynn A Fairbanks, Susan O'Connor, Susan Rosenberg, and Jeffrey L Cummings. 2001. Activities of daily living in Alzheimer's disease: neuropsychiatric, cognitive, and medical illness influences. *The American Journal of Geriatric Psychiatry* 9, 1 (2001), 81–86.
- [58] Yonglong Tian, Chen Sun, Ben Poole, Dilip Krishnan, Cordelia Schmid, and Phillip Isola. 2020. What makes for good views for contrastive learning. *arXiv preprint arXiv:2005.10243* (2020).
- [59] Linlin Tu, Xiaomin Ouyang, Jiayu Zhou, Yuze He, and Guoliang Xing. 2021. Feddl: Federated learning via dynamic layer sharing for human activity recognition. In *Proceedings of the 19th ACM Conference on Embedded Networked Sensor Systems*. 15–28.
- [60] Yancheng Wang, Yang Xiao, Fu Xiong, Wenxiang Jiang, Zhiguo Cao, Joey Tianyi Zhou, and Junsong Yuan. 2020. 3dv: 3d dynamic voxel for action recognition in depth video. In *Proceedings of the IEEE/CVF conference on computer vision and pattern recognition*. 511–520.
- [61] Lu Xia and JK Aggarwal. 2013. Spatio-temporal depth cuboid similarity feature for activity recognition using depth camera. In *Proceedings of the IEEE conference on computer vision and pattern recognition*. 2834–2841.
- [62] Huatao Xu, Pengfei Zhou, Rui Tan, Mo Li, and Guobin Shen. 2021. LIMU-BERT: Unleashing the Potential of Unlabeled Data for IMU Sensing Applications. In *Proceedings of the 19th ACM Conference on Embedded Networked Sensor Systems*. 220–233.
- [63] Yasunori Yamada, Kaoru Shinkawa, Masatomo Kobayashi, Vittorio Caggiano, Miyuki Nemoto, Kiyotaka Nemoto, and Tetsuaki Arai. 2021. Combining multimodal behavioral data of gait, speech, and drawing for classification of Alzheimer's disease and mild cognitive impairment. *Journal of Alzheimer's Disease* 84, 1 (2021), 315–327.
- [64] Hanbin Zhang, Gabriel Guo, Chen Song, Chenhan Xu, Kevin Cheung, Jasleen Alexis, Huining Li, Dongmei Li, Kun Wang, and Wenyao Xu. 2020. PDLens: Smartphone Knows Drug Effectiveness among Parkinson's via Daily-Life Activity Fusion. In *Proceedings of the 26th Annual International Conference on Mobile Computing and Networking (MobiCom '20)*. Association for Computing Machinery, New York, NY, USA, Article 12, 14 pages. <https://doi.org/10.1145/3372224.3380889>
- [65] Yuchen Zhao, Payam Barnaghi, and Hamed Haddadi. 2022. Multi-modal Federated Learning on IoT Data. In *2022 IEEE/ACM Seventh International Conference on Internet-of-Things Design and Implementation (IoTDI)*. IEEE, 43–54.
- [66] Yue Zhao, Meng Li, Liangzhen Lai, Naveen Suda, Damon Civin, and Vikas Chandra. 2018. Federated learning with non-iid data. *arXiv preprint arXiv:1806.00582* (2018).